TENSILE FRACTURE AND CREEP-RUPTURE BEHAVIOR OF SiC FIBERS

Hee Mann Yun and James A. DiCarlo

NASA Glenn Research Center, Cleveland, Ohio 44135

ABSTRACT

In order to better understand the fiber role for fracture and rupture of SiC fiber-reinforced ceramic matrix composites (CMC), mechanical tests were performed on single filaments, multifilament tows, and multi-tow fabrics of different types of SiC fibers: near-stoichiometric Hi-Nicalon Type S, Tyranno SA, Sylramic, Sylramic-iBN, and non-stoichiometric Hi-Nicalon and Tyranno ZMI. All fibers were sized with a low molecular weight polymer, and also were tensile fracture tested after coating with a thick and compliant layer of BN. Creep-rupture data were obtained at 1400°C in air and in argon. For the near-stoichiometric SiC tow and fabric with rough surfaces, the sizing and coating significantly affected the room temperature tensile fracture characteristics. Based on simple bundle theory, measured tensile fracture strengths for sized tows, coated tows, and fabrics of all fiber types were in general agreement with the single fiber results. Even though the final fracture behavior and strength properties of some fiber types showed strong effects on the testing environments and fiber specimen form, the initial surface flaw that was introduced during fiber fabrication and the creep-induced cavity growth by stress and time were the most crucial factor for the as-produced room temperature tensile strengths and the high-temperature creep-rupture. In this regard, the treated Sylramic-iBN and Hi-Nicalon Type S fibers showed the best fracture and rupture resistant behavior.

KEYWORDS

SiC fiber, SiC fabric, SiC/SiC composite, tensile fracture, creep rupture

INTRODUCTION

Continuous silicon carbide (SiC) fibers have been developed for reinforcement of ceramic matrix composites (CMC) for high temperature structural components. Small diameter SiC fibers produced by polymer pyrolysis possess high stiffness, high room temperature strength, and high thermal stability. The near-stoichiometric Sylramic fiber and the non- stoichiometric Hi-Nicalon fiber (excess carbon and trace oxygen) are leading candidates for high temperature CMC because they have displayed thermostructural behavior superior to that of the high-oxygen containing Nicalon SiC fiber [1,2]. In contrast to non-stoichiometric SiC fibers, the Sylramic fiber showed no weight loss, grain growth, or contraction below 1500°C. The Hi-Nicalon Type S and Tyranno SA are other near-stoichiometric fibers, whose grain sizes and tensile strengths are similar to those of the Sylramic fiber. More recently, improved tensile and creep-rupture behavior have also been achieved for the Sylramic-iBN fiber, which is derived from the Sylramic fiber by special developmental processes that yield microstructures with smaller boron content [3]. Thus there exists various process routes and microstructural possibilities for thermally stable stoichiometric SiC

fibers.

The properties of the small-diameter SiC fibers are typically measured using single fibers removed from multifilament tows containing ~400 to 1600 fibers. However, since CMC are almost always constructed using woven or braided tows, mechanical tests on either coated and/or uncoated tightly-packed multifilament tows or even woven fabrics that have been exposed to simulated CMC process and service conditions should be more useful for understanding fiber performance within CMC than single fiber tests. These tow or fabric tests not only allow the evaluation of many fibers in the structural forms used in CMC, but also permit a better understanding of the various fiber surface and load transfer interactions that may occur within the CMC. The objective of this study was therefore to understand SiC fiber performance in CMC by measuring the tensile strength and creep-rupture properties of multifilament tows and fabrics consisting of various non-stoichiometric and stoichiometric SiC fibers.

EXPERIMENTAL PROCEDURE

Six types of SiC fibers available as continuous-length multifilament tows were examined: the non-stoichiometric Hi-Nicalon and ZMI fibers, and the stoichiometric Hi-Nicalon Type S, Tyranno SA, Sylramic, and Sylramic-iBN fibers. This last fiber not only has less boron content in the fiber bulk than the precursor Sylramic fiber, but also has a thin (~150 nm) crystalline BN layer on the fiber surface [4]. Table 1 lists typical properties of all the fiber types. In the as-produced condition, the tows for each type were sized with a polymer-based material (see Table 1). These tows were then utilized to fabricate 0/90-degree satin weave fabric by a commercial weaving vendor. This fabric is the basic fiber structure used in most commercial CMC today [5]. For fabric testing, specimen strips, ~13mm wide (10 tows) and ~150mm long, were cut from the fabric cloth and mounted onto paper tabs. Detailed procedures for tow and fabric preparation and testing are reported elsewhere [6]. To determine tensile strength, all fiber types were tested to fracture at room temperature using a 25 mm grip to grip length and a constant displacement rate of 1.27 mm/min. The average cross-sectional area for the multifilament specimens was assumed to be equal to the filament-count times the average fiber area based on the average diameter for each type. The creep-rupture properties were determined for tows and fabrics using the same fiber creep-rupture facilities and procedures previously reported on the single fiber [6]. Creep deformation versus time was recorded at a constant deadweight load using either 25mm or 100mm hot zone lengths for the air furnace.

RESULTS AND DISCUSSION

The room-temperature tensile strengths are shown in Fig. 1 for (a) single fibers, (b) tows, and (c) woven fabrics in their as-produced condition, either sized or BN coated, and after exposure at 1000°C for 3 hours in vacuum or at 1400 °C for 1 hour in argon. These exposure conditions were chosen to simulate those typical of interphase and matrix formation, respectively, for current SiC/BN/SiC composites [7]. Fig. 1a shows that the average tensile strength for the as-processed Sylramic, Syl-iBN, and ZMI single fibers were the highest, above 2700 MPa; while those of the SA and Hi-Nicalon-S fibers were below 1900 MPa. The low strength of the SA fiber is due to mainly large initial flaws that could be related to the fact that it has the largest grain size among all fibers. After inert exposure, the average strengths of single fibers from all fiber types decreased. The degree of degradation is strongly dependent on the type and content of impurities on its surface plus the chemical composition of the exposure environment. This strength degradation under inert conditions is due to changes in the fiber surface morphologies and chemistries by the exposure environment [8].

In general, the average strengths of single tows, as shown in Table 2 and Fig. 1b, were either lower or in good agreement with those of the 10-tow fabrics (Fig. 1c); and the strength ranking for different fiber types was similar to that of the single fiber. The highest tow and/or fabric strength was ~1800 MPa for the Sylramic and Hi-Nicalon fibers; while the lowest was ~500 MPa for the SA fiber. The coated tows showed a similar strength to the as-produced/sized tows. As with single fibers, strengths of multifilament fibers in forms of

tow or fabric also decreased after exposures at 1000°C, and decreased further at 1400°C with some types losing, up to 50 % of their initial strengths.

To better understand the strength of the as-produced multi-fibers, it can be assumed that the individual fibers fractured independently, so that multi-fiber strengths could be calculated using the single fiber results and simple bundle theory assuming the same gauge length of 25 mm [9]:

$$\sigma_b / \sigma_f = (1/(m\,e))^{(1/m)} / \Gamma((m+1)/m) \quad (1)$$

Here σ_b is the predicted multi-fiber bundle strength, σ_f is the average measured strength for the single fibers, **e** is the natural logarithm base, Γ is the gamma function, and **m** is the Weibull modulus that characterizes the strength distribution of the single fibers. For each SiC fiber type in the as-produced condition, Table 2 shows the calculated and the measured average multi-fiber strength using the Weibull modulus and average strength for the single fibers, and assuming the same gauge length of 25mm. In Table 2, it can be seen that the measured and predicted fabric strengths were generally agreed to the predicted. This was probably due to fabric gauge length being smaller than the grip-to-grip length due to the initial 90-degree tow. However, some as-produced tow with no inter-laced tow showed lower strengths than expected from simple bundle theory, suggesting that the fibers within the tows did not fracture independently. Two possible mechanisms for non-independent fracture are (1) fiber-fiber interaction due to mechanical abrasion and (2) fiber-fiber interaction due to chemical bonding. In both cases, the fracture of the weaker fibers causes premature fracture of the stronger fibers, resulting in a reduced strength for the multi-fiber specimens. The lower tow and fabric strengths for the near-stoichiometric Sylramic and Syl.-iBN fibers with rough surfaces and for the SA fiber with excess sizing can be explained by mechanisms 1 and 2, respectively (see Table 1). Both mechanisms could also explain the loss in multi-fiber strengths after the inert treatments since removal of the fiber sizings may result in more fiber-fiber abrasion and changes in the BN-coatings may result in fiber-fiber chemical bonding.

After air exposure for 100 hours from 400 to 1000°C, room-temperature tow and fabric strengths decreased as shown in Fig. 2a for the stoichiometric SiC fibers, and Fig. 2b the non-stoichiometric fibers, and also included the CVI-BN coated fibers. The air exposures were used to simulate effects from CMC cracking under oxidizing service conditions and from CMC fabrication conditions in which the tows are inadvertently exposed to oxygen, such as during BN interphase deposition at intermediate temperatures. Typically the tow strengths for all fiber types, including the coated fibers, started to drop at ~200°C, and then leveled off at ~ 600°C to ~50 to 80% of their as-produced strengths. Near 1000°C, the strengths of all tows dropped to about the same low level of <~400 MPa. The BN-coated tows appeared to degrade at even lower temperatures, indicating easier fiber-fiber bonding because of tight tows and boron-enhanced silica formation on the fiber surfaces. Contrary to the tows, which have loosely touching fibers during air exposure, the fabrics with tight tows due to interlacing displayed a more rapid strength loss with temperature, so that near 600°C, the strengths of all fabrics dropped to about the same low level of <~400 MPa, nearly 10% of their as-produced values. However, the Syl.-iBN fabric degraded only to a level of ~2/3 of its initial strength. The developmental Syl.-iBN fiber with reduced boron and a crystalline BN surface appears to measurably reduce oxidation-induced bonding at intermediate temperatures. For the Hi-Nicalon fiber, previous TGA studies [4] suggest that the sharp strength drop from ~500 to 600°C were probably due to oxidative removal of sizing and perhaps intrinsic carbon on the fiber surface. The intrinsic carbon on the Hi-Nicalon may have not only healed surface flaws, but also allowed compliant interaction between fibers. For the other tow fiber types, strength degraded slowly in a continuous manner up to ~800°C. For the Sylramic tow, the small increase in strength near 900°C appears to be caused by the formation of a borosilicate glass surface layer which, if thin enough, appears to be able to heal surface flaws without chemically bonding the fibers together. Indeed, due to the presence of boron and TiB_2 on the fiber surface [9], larger TGA weight increases were observed at intermediate temperatures for the Sylramic fiber [5]. Above 1000°C, all tow fibers began to rapidly form silica on their surfaces, which effectively bonded all the fibers together. This gives rise to tow strengths of <~400 MPa.

In support of a chemical bonding issue during multi-fiber air exposures, the general fracture surfaces for the

low strength tows showed (1) localized failure with many groups of fibers bonded together and (2) one or more fracture planes depending upon degree of fiber-fiber bonding. Typical fracture surfaces for the Hi-Nicalon and Sylramic fibers, tow and fabric, are shown in Figs. 3a and 3b before and after a 700°C air exposure, respectively. The single fibers, not shown here, before and after exposure showed no significant alteration of the fracture origin, mainly surface flaws. The tow and fabric fracture surfaces showed two different types: either a bulged explosion style fracture with independent fiber fracture, or a bonded non-explosion style fracture with correlated fiber fracture. The fracture surfaces of the fabric specimens changed from an independent to the dependent fracture mode after air exposure. For CMC, the oxidation results clearly point to the need for some fiber separation within woven tows, plus minimal contamination with oxygen during the interphase coating process or during composite application.

Plots of applied stress versus average rupture time are shown in Fig. 4 for Hi-Nicalon and Sylramic tows and single fibers at 1400°C in (a) air and (b) argon for the as-produced and BN-coated conditions. The time rate of rupture strength degradation for the tows was much weaker than that for the single fibers. The degradation rate for the BN-coated specimens was more rapid than that of the un-coated specimens. At short times (or high stresses), the Hi-Nicalon and Sylramic tows displayed lower rupture strengths (or shorter rupture times) than the single fibers. At long times (or low stresses), the un-coated tows displayed higher rupture strengths (or longer rupture times) than the single fibers or coated tows. Also shown in Fig. 5 is the rupture strength behavior of single Syl.-iBN fibers, which is significantly different in air and argon. In air, this fiber type shows reduced creep and the most rupture-resistant behavior observed to date for all SiC fiber types [11]. Apparently in air, oxide formation allows better creep resistance and blunts strength controlling flaws on the Sylramic-iBN fiber surfaces; while in argon, creep is enhanced and flaw blunting by silica formation is not available. The exact mechanisms for these environmental effects are still unknown. Thus, the general trends observed at 1400°C, which also occurred at 1200°C, are currently creating difficulties for understanding the creep-rupture behavior not only of tows and fabrics, but also of single fibers.

SUMMARY AND CONCLUSIONS

Tensile strengths of as-produced tows or fabric specimens containing various types of SiC fibers can be predicted in most cases by bundle theory in which it is assumed that all fibers fracture independently. In those cases where the measured strengths were lower than predicted, effects due to adverse fiber-fiber mechanical and chemical interactions appeared to be existent. These issues became more prevalent after multi-fiber tow and fabric specimens were subjected to inert thermal treatments or to air exposures at intermediate temperatures. TGA studies suggest that the primary strength degradation mechanism was sizing removal for the inert treatment, and fiber-fiber bonding by surface oxide growth and surface carbon layer removal for the air treatments. Contrary to the room-temperature strength results, the high temperature creep-rupture strengths of tows and fabrics were generally higher than those of single fibers, with environmental effects playing a strong role. Clearly more studies are needed to understand the high-temperature creep-rupture results.

REFERENCES

(1) J.A. DiCarlo and S. Dutta: Continuous Ceramic Fibers for Ceramic Composites. HANDBOOK ON CONTINUOUS FIBER REINFORCED CERAMIC MATRIX COMPOSITES, eds. R.Lehman, S.El-Rahaiby, and J.Wachtman, Jr., Ceramic Information Analysis Center, Purdue University, West Lafayette, Indiana, 1995.

(2) K. Okamura,"Ceramic Fibers from Polymer Precursors", Composites, **18**, 2, 1987, pp 107-120.

(3) H.M. Yun and J.A. DiCarlo, unpublished work, 1997.

(4) H.M. Yun and J.A. DiCarlo, "Comparison of the Tensile, Creep, and Rupture Strength Properties of Stoichiometric SiC Fibers", NASA TM 209284, 1999.

(5) J.A. Dicarlo and H.M. Yun: "Fiber Test Development for Ceramic Composite Thermomechanical properties", ASTM STP 1392, 1999, edited by M.G. Jenkins, E.L-Curzio, and S.T. Gronczy.

(6) H.M. Yun and J.A. DiCarlo, "Thermomechanical Behavior of Advanced SiC Fiber Multifilament Tows", Cer. Eng. and Sci. Proceedings, 17A, 1996, pp. 61-67.

(7) D. Landini and P. Gray: private communications to HACI, 1999.

(8) F. Rebillat, A. Guette, L. Espitalier, and R. Naslain, "Chemical and Mechanical Degradation of Hi-Nicalon and Hi-Nicalon S Fibers under CVD/CVI BN Processing Conditions", HIGH TEMPERATURE CERAMIC MATRIC COMPOSITES III, The Ceramic Society of Japan, 1998, pp 31-34.
(9) B.W. Rosen, "Thermomechanical Properties of Fibrous Composites", Proc. Roy. Soc. Lond. A. 319, 1970, pp. 79-94

Table 1. NOMINAL PROPERTIES OF SiC FIBERS

Trade Name	Hi-Nicalon	ZMI	Hi-Nicalon S	SA	Sylramic	Syl.-iBN
	non-stoichiometric SiC		near-stoichiometric SiC (C/Si~1.0)			
Manufacturer	Nippon Carbon	Ube Industries	Nippon Carbon	Ube Industries	Dow Corning	Dow Corning + NASA
Avg. Grain Size, nm*	4(XRD)	-	22 (XRD)	>~150	~ 100	~ 100
Second Phases or Impurity Conc.(wt.%)	0.5 O, 36 C	8.3 O, 35 C, 2 ZrX	O(0.2)	Al(<2), O(0.3)	TiB2, B	Reduced B, TiB2, B-N
Avg. Diam., μm	14	11	13	10	10	10
# of Filaments per tow	500	400	500	800	800	800
PVA Sizing, wt.%	>1	(~1.0)#	1.2	(~1.0)#	~0.2	-
Modulus at RT GPa)	270	200	400-420	375	~400	> 400
Tensile Strength, MPa	2800	2700	~2500	2800	3200	~3200
Tensile Elongation, %	~1.0	1.7	~0.6	~0.7	~0.8	<~0.8

*MEASURED ON TEM MICROSTRUCTURES, # PEO SIZING

Table 2. Strength Characteristics of SiC Single Fibers, Tows, and Fabrics

Fiber Type	Avg. tensile strength (MPA) at room temperature, As-Produced Condition				
	Single Fibers	(m)	Tows	Fabrics	Predicted Tow Strength*
Hi-Nic.	2240	6	1960	2200	1520
ZMI	2700	5	1770	-	1740
Hi-Nic. S	1900	3	1450	1610	1060
SA	1430	3	280	1340	800
SYLRAMIC	2800	4	1550	1850	1700
SYL.-iBN	3060	4	1270	1840	1860

* PREDICTED BY BUNDLE THEORY, Eq. (1), + NO SIZING

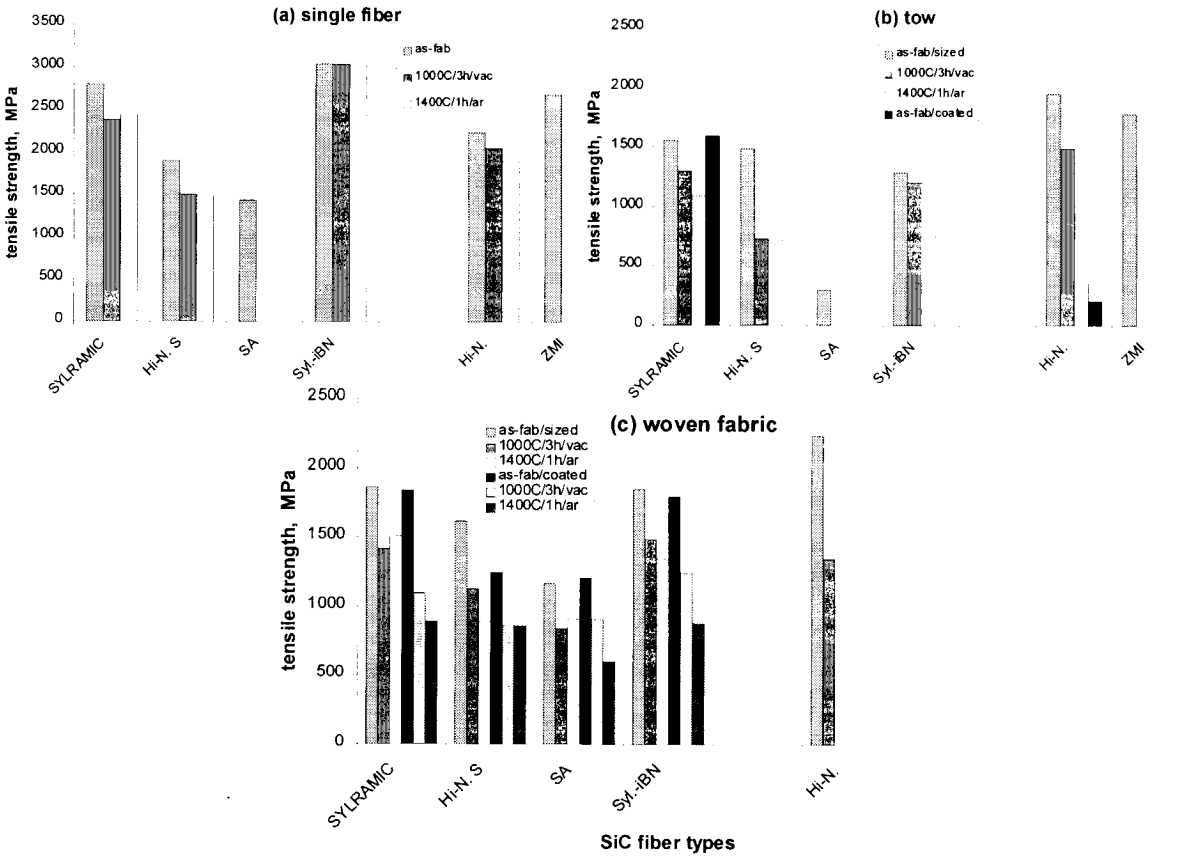

Fig. 1 Tensile fracture strength of SiC fibers, as-fabricated and BN-coated

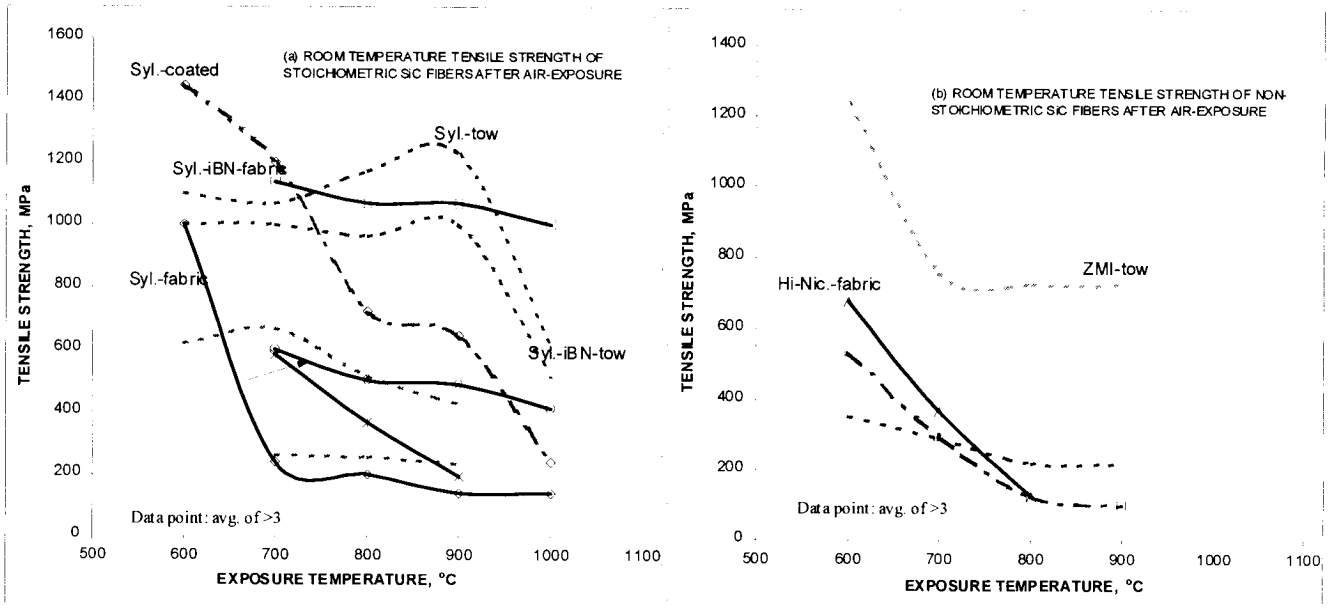

Fig. 2 Retained tensile fracture strength of SiC fibers after 100hr-air exposure.

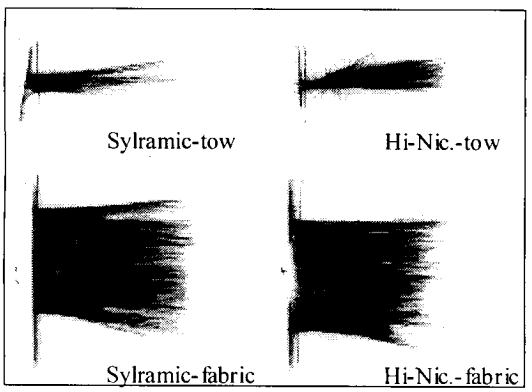

(a) R.T. tensile fracture, as-fabricated

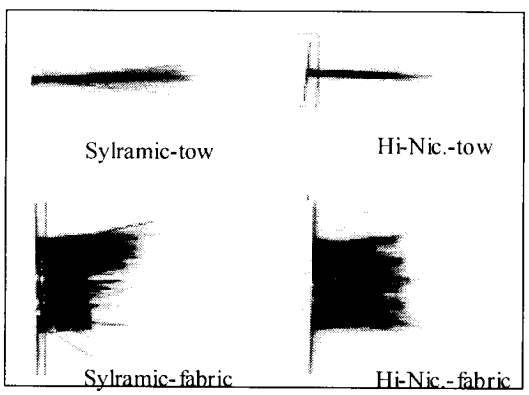

(b) R.T. tensile fracture after 700C/100hr/air exposure

Fig. 3 Typical tensile fracture surfaces of dependent and independent fiber failures.

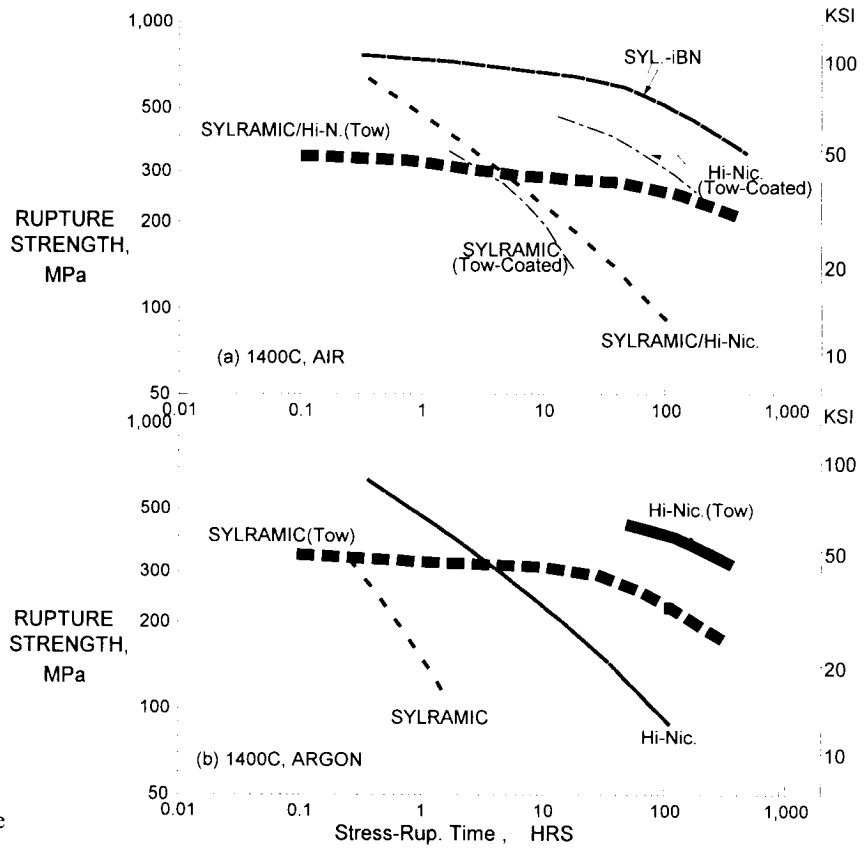

Fig. 4 1400 C creep-rupture strength of SiC fibers, tested in (a) air and (b) argon